Journal of Solid State Chemistry **151,** 220–224 (2000)
doi:10.1006/jssc.2000.8642, available online at http://www.idealibrary.com on IDEAL®

Sodium Ordering in $Na_xW_{18}O_{49}$

A. Martínez-de la Cruz,*,[1] Leticia M. Torres-Martínez,* F. García-Alvarado,† E. Morán,‡ and M. A. Alario-Franco‡

*Facultad de Ciencias Químicas, División de Estudios Superiores, Universidad Autónoma de Nuevo León, Apartado Postal 1625, Monterrey, N.L., Mexico; †Facultad de Ciencias Experimentales y Técnicas, Universidad San Pablo-CEU, Urb. Montepríncipe, Apd. Correos 67, 28668 Boadilla del Monte, Madrid, Spain; and ‡Departamento de Química Inorgánica, Facultad de Ciencias Químicas, Universidad Complutense, 28040 Madrid, Spain

Received November 8, 1999; in revised form January 21, 2000; accepted January 26, 2000

Sodium insertion in $W_{18}O_{49}$ proceeds through the formation of a solid solution for the whole range of intercalant $Na_xW_{18}O_{49}$ with $0 \leq x \leq 1.8$. The different features detected in $-\partial x/\partial E$ vs E plots have been associated with continuous phase transitions. In order to know more about these transitions, several samples $Na_xW_{18}O_{49}$ with compositions around the minimum in the $-\partial x/\partial E$ curve have been synthesized and then characterized by both X-ray and electron diffraction techniques. An interesting correlation with the electrochemical results has been established.

Key Words: **sodium insertion; order–disorder transitions; insertion in tungsten oxides.**

INTRODUCTION

Many insertion compounds have been studied to date due to their possible use as electrodes in rechargeable lithium batteries or as active material in electrochromic devices (1). The performance of the materials in these electrochemical devices depends on the characteristics of the insertion reaction. In this sense, several electrochemical techniques have been developed (2–4) to study the nature of the reaction. The voltage–composition plot provides very valuable information about the thermodynamic features of an insertion system. Thus, in a single-phase solid solution domain, continuous transitions are sometimes observed, and potential continuously varies with the composition whereas in the two-phase domains the voltage is constant, since the transformation of one phase into another can be considered a first-order transition.

In 1979 Thompson (4) introduced the term *incremental capacity* ($-\partial x/\partial E$) to detect, with high resolution, the different processes that occur during an insertion reaction. This is in fact possible since some features in the $-\partial x/\partial E$ vs E diagram can be associated with either first-order or continuous transitions (5, 6).

In recent years, a powerful electrochemical technique to characterize the insertion process has been developed: *step potential electrochemical spectroscopy* (SPECS) (7–9). By applying a potential to the system and recording the current relaxation versus time in each potential step, the nature of the different processes that take place during the insertion can be deduced. Taking into account this information, we can build a *phase diagram* of the insertion system.

In this paper, a study of $Na_xW_{18}O_{49}$ is presented. The oxide $W_{18}O_{49}$ has a structure that can be described as pairs of pentagonal columns linked by an edge-sharing octahedron. These pairs are then connected to another octahedron along the *a*- and *c*-directions. The short axis, *b*, has the length of the cubic perovskite lattice parameter as the octahedron is sharing corners along that direction (10, 11). Figure 1 shows the arrangement of tungsten and oxygen atoms. This W–O framework produces three different types of empty tunnels. These are, respectively, hexagonal (labeled *h*), quadrangular (labeled *q*), and triangular tunnels (labeled *t*).

Following our previous work on lithium insertion in $W_{18}O_{49}$ (12, 13) we have performed the electrochemical insertion of sodium in this oxide. Features in the E–x diagram have been studied in detail by SPECS and several samples $Na_xW_{18}O_{49}$ have also been both synthesized and characterized by X-ray diffraction and electron microscopy.

EXPERIMENTAL

The synthesis of $W_{18}O_{49}$ was carried out by solid-state reaction of WO_3 and W, mixed in the appropriate stoichiometric ratio. Fresh WO_3 was obtained by the decomposition of H_2WO_4 at 850°C for 3 days. The mixture was ground and placed in a quartz tube that was then evacuated, sealed, and heated at 1000°C for 3 days. Structural characterization of $W_{18}O_{49}$ and $Na_xW_{18}O_{49}$ samples

[1] To whom correspondence should be addressed. Fax: (52) 8 374-49-37. E-mail: azmartin@ccr.dsi.uanl.mx.

0022-4596/00 $35.00

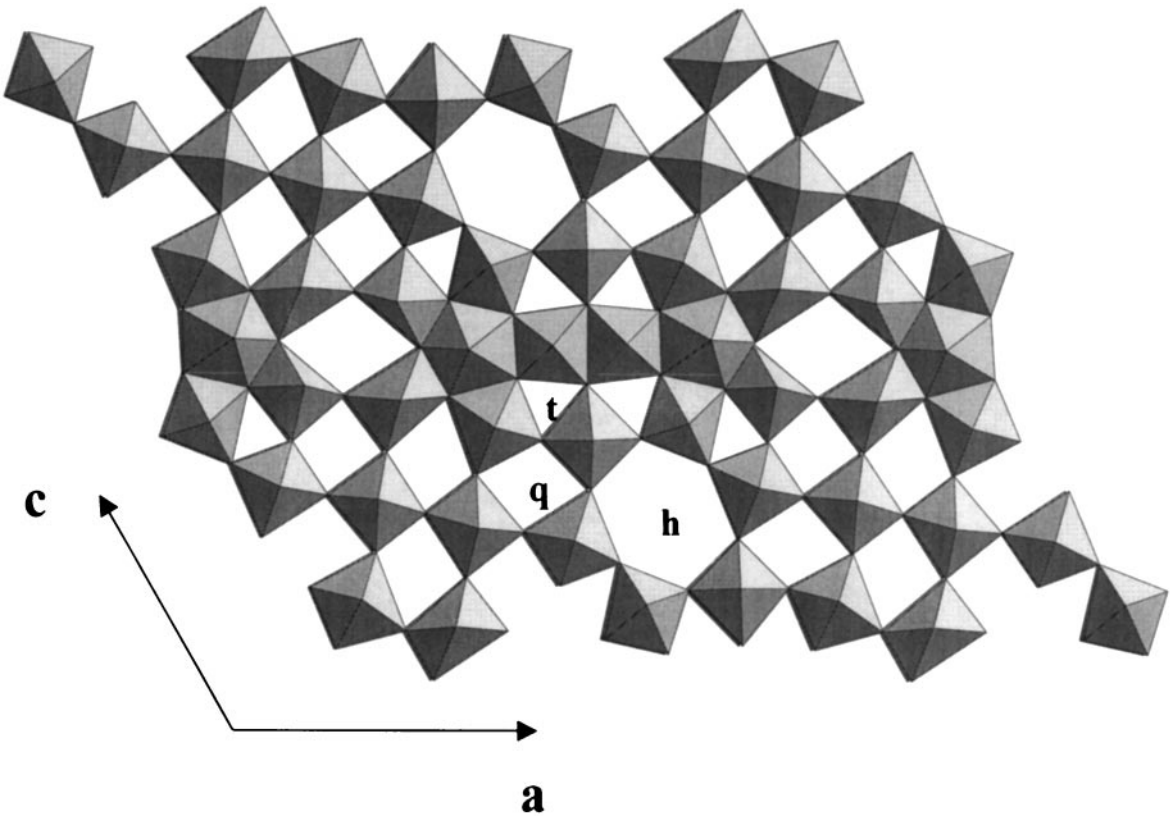

FIG. 1. Schematic representation of the $W_{18}O_{49}$ structure. Three different types of tunnels (triangular, quadrangular, and hexagonal) are present.

was carried out by X-ray diffraction techniques using a SIEMENS D-5000 diffractometer with Cu$K\alpha$ ($\lambda = 1.5418$ Å). The insertion compounds $Na_xW_{18}O_{49}$ were also characterized by electron diffraction techniques using a JEOL 2000FX electron microscope.

Electrochemical insertion was performed using a multichannel galvanostat/potentiostat of the MacPile type. For the experiments, Swagelok-type cells (14) using sodium as the negative electrode were assembled. As the electrolyte, a 1 mol dm^{-3} solution of $NaClO_4$ in propylene carbonate (PC) was used. Under potentiostatic conditions, SPECS experiments were run at a sweep rate of ± 10 mV/20 h. The cells used contained pellets with around 200 mg of active material as the positive electrode, carbon black, and ethylene–propylene–diene terpolymer (EPDT) in a 90:9:1 ratio.

The sodium diffusion coefficient was determined using the potentiostatic method (3). In this work, we have estimated the surface area of the active material assuming that grains are spherical with a diameter equal to the average particle size. The particle size of $W_{18}O_{49}$ was measured using a Malvern-type Master SizerX analyzer as described in more detail in Ref. (15). All the electrochemical experiments were made under isothermal conditions (35°C $\pm$ 0.2°C) in order to avoid temperature effects in the electrochemical measurements.

The synthesis of samples of $Na_xW_{18}O_{49}$, for structural characterization, was carried out by electrochemical insertion methods under potentiostatic conditions. Several cells were discharged with a voltage scanning rate of ± 10 mV/h until predetermined values of x. When the condition $|I| < |I_o|/1000$ was satisfied, the step duration was interrupted and then the next voltage step was applied. In order to obtain impurity-free samples, the cathode composition was 100% of active material. In order to avoid any possible reaction with moisture all operations in which these insertion compounds were involved were carried out in an argon atmosphere.

RESULTS AND DISCUSSIONS

When sodium is electrochemically inserted in $W_{18}O_{49}$ the voltage of the cell $Na/NaClO_4$ (1 mol dm^{-3}) + $PC/W_{18}O_{49}$ varies with composition as shown in Fig. 2. The complete charge–discharge cycle shows the reversibility of the insertion process in the range between 3.3–1.0 V vs Na^+/Na^0. It is important to note that below 1.0 V more than 2 Na^+/ formula can be reached, although the reaction is irrevers-

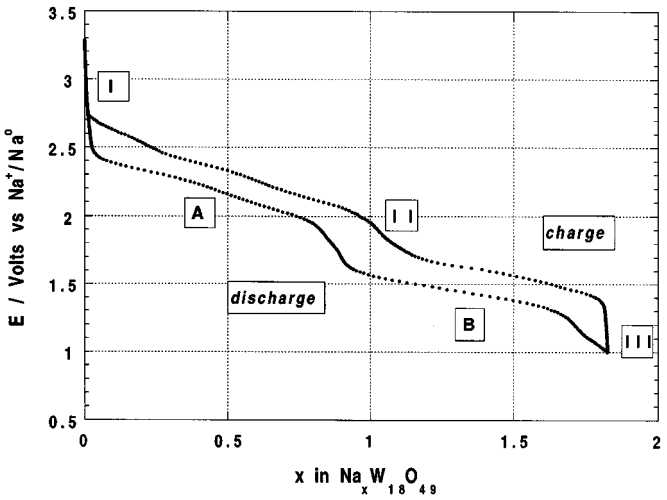

FIG. 2. Voltage–composition plot obtained from potentiostatic cycling of a cell $Na//W_{18}O_{49}$.

ible. Sodium insertion in $W_{18}O_{49}$ proceeds through different processes as can be deduced from the different slopes of cell voltage variation with sodium content: abrupt voltage variations for regions labeled I, II, and III, and more constant for regions labeled A and B.

In order to know more about the origin of these processes, we have analyzed in more detail the information obtained from the SPECS experiment. In this way, after studying the current relaxation with time at every voltage step we deduced that $Na_xW_{18}O_{49}$ behaves in the range $x = 0$–1.8 as a solid solution. Figure 3 shows a chronoamperogram for a cell with configuration $Na/W_{18}O_{49}$ that was discharged with a very low scanning voltage rate, -10 mV/20 h. It is important to note that the voltage was kept in every step while the condition $|I| > |I_o|/100$ was satisfied. For high potential values, at the beginning of the insertion reaction only small currents are detected and the cell exhibits a low capacity (region I). Below ~ 2.45 V the cell exhibits a high capacity (regions A and B), excepts in the regions labeled II and III, where again a low increase of capacity is observed. As shown in the chronoamperogram, in every range of composition the current decays to zero before the next voltage step is applied. Hence we deduced that the diffusion of sodium ions is the mechanism that rules the intercalation reaction in the whole range of composition. Taking this into account, we said above that sodium is inserted in $W_{18}O_{49}$ through a single-phase solution in all ranges of composition ($0 \leq x \leq 1.8$). Then the different processes detected along the solid solution formation are associated with continuous phase transitions. In agreement with this, when samples with different composition, but belonging to the same range of solid solution, were examined by X-ray diffraction, their diffraction pattern showed only a slight peak shift to lower angles.

Formations of continuous phase transitions have been studied with high accuracy in early work (5, 16–18) through incremental capacity measurements ($-\partial x/\partial E$). In this way, when the incremental capacity is plotted versus the cell potential (or composition) for the system $Na/W_{18}O_{49}$, several maxima in the $-\partial x/\partial E$ values are detected, see Fig. 4. In fact, we can see that a new process is present near $x = 0.5$. It corresponds to a soft slope change in the E–x plot. In the same way, the accuracy of the measurement allows us to see that the process labeled II, where E abruptly drops as x increases, is in fact formed by two consecutive processes. Following the lattice gas model proposed by McKinnon *et al.* (5, 6) for some intercalation systems, the different peaks observed in $-\partial x/\partial E$ should correspond to phase

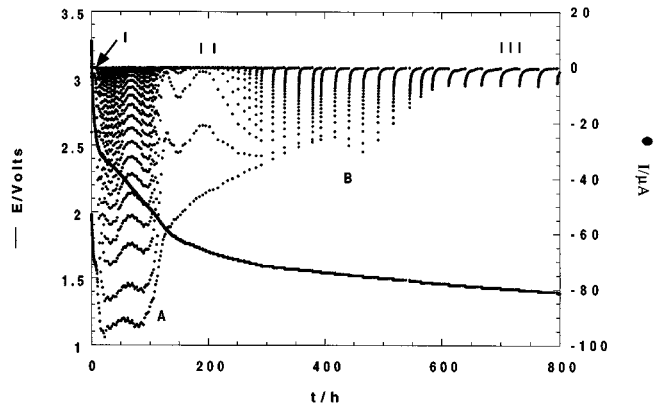

FIG. 3. Variation of intensity current with time during the different voltage steps (± 10 mV/20 h) of a potentiostatic experiment. The cell $Na//W_{18}O_{49}$ was kept at 35 ± 0.2°C to avoid temperature effects in the current relaxation.

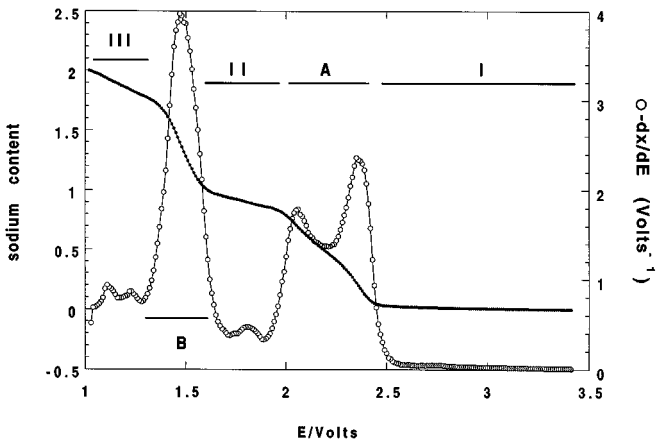

FIG. 4. Variation of incremental capacity ($-\partial x/\partial E$) during the discharge of a cell $Na//W_{18}O_{49}$.

transitions between the ordered and disordered states that take place as x is varied. On the other hand, the minima should correspond to the particular compositions at which a new ordering structure is obtained. To confirm whether the model effectively applies to our system, we have synthesized different samples $Na_xW_{18}W_{49}$ ($x = 0.25, 0.45, 0.82, 0.9, 1.5$, and 1.8) through the discharge of electrochemical cells. Figure 5 shows two typical electron diffraction patterns of samples whose compositions are close to two different minima in the $-\partial x/\partial E$ plot, $Na_{0.45}W_{18}O_{49}$ and $Na_{0.82}W_{18}O_{49}$. These patterns could not be indexed on the basis of the original cell of $W_{18}O_{49}$ due to the presence of extra spots (see white arrow). Nevertheless, both patterns, together with some more that are not shown here, can be fully indexed using a cell $a \times b \times 2c$ times that of $W_{18}O_{49}$. The formation of a superstructure along the c-axis may be an indication of a new sodium ordering that would be in agreement with our first interpretation, above, of the features observed in the $-\partial x/\partial E$ plot and the I–t diagram. Although many different crystals were examined the a- and b-axes were never observed to be affected.

On the other hand, when samples with compositions belonging to the other minima were studied, i.e., $Na_{0.9}W_{18}O_{49}$ and $Na_{1.8}W_{18}O_{49}$, some streaking was observed. This seems to suggest the existence of some incipient ordering also for these compositions. However, we did not succeed in obtaining the corresponding ordering states.

Electron diffraction in samples with compositions close to the minima reveal effects related to ordering–disordering situations. In contrast, when samples with compositions near the different maxima in the $-\partial x/\partial E$ plot were analyzed, all diffraction patterns could be indexed on the basis of a $W_{18}O_{49}$ cell. There is then a clear agreement between the two approaches to the study of the ordering.

Although the details of ordering have not yet been determined for the different $Na_xW_{18}O_{49}$ ordered compositions, some assumptions can be made. Taking into account the ionic radius of Na^+ (for example, $r^{VI} = 1.02$ Å to $r^{XII} = 1.39$ Å) (19) and the maximum quantity of sodium inserted, sodium insertion may proceed by the filling of the unique hexagonal tunnel present in $W_{18}O_{49}$. Although triangular tunnels seem to be very small to accommodate a sodium ion, the incorporation of sodium could also take place in the quadrangular tunnel. However, if this were fully occupied it would lead to a minimum composition of $Na_7W_{18}O_{49}$. On the other hand, as reported in early work in related systems (20), sodium ions mainly occupy tunnels that are larger than the quadrangular ones, such as pentagonal or hexagonal tunnels for example.

Diffusion coefficients have been determined in the whole range of existence of the solid solution. When the insertion proceeds in the range $W_{18}O_{49}$–$Na_{0.7}W_{18}O_{49}$, the sodium diffusion coefficient, D_{Na^+}, takes values of the order of 10^{-9} cm^2 s^{-1}, and is essentially independent of x. However, the situation is very different in the range of composition $Na_{0.9}W_{18}O_{49}$–$Na_{1.6}W_{18}O_{49}$: an abrupt drop in the sodium diffusion coefficient occurs in this range, and now it takes values between 10^{-10}–10^{-11} cm^2 s^{-1} as x increases. It then appears that the presence of two sodium ions inserted in the hexagonal tunnel, in accordance with our insertion model, is at the origin of this decreasing. In fact the multioccupancy by sodium ions of the large tunnels, such as the hexagonal ones, has been used before to explain the maximum sodium insertion in h-WO_3, 0.67 sodium ions per formula (21).

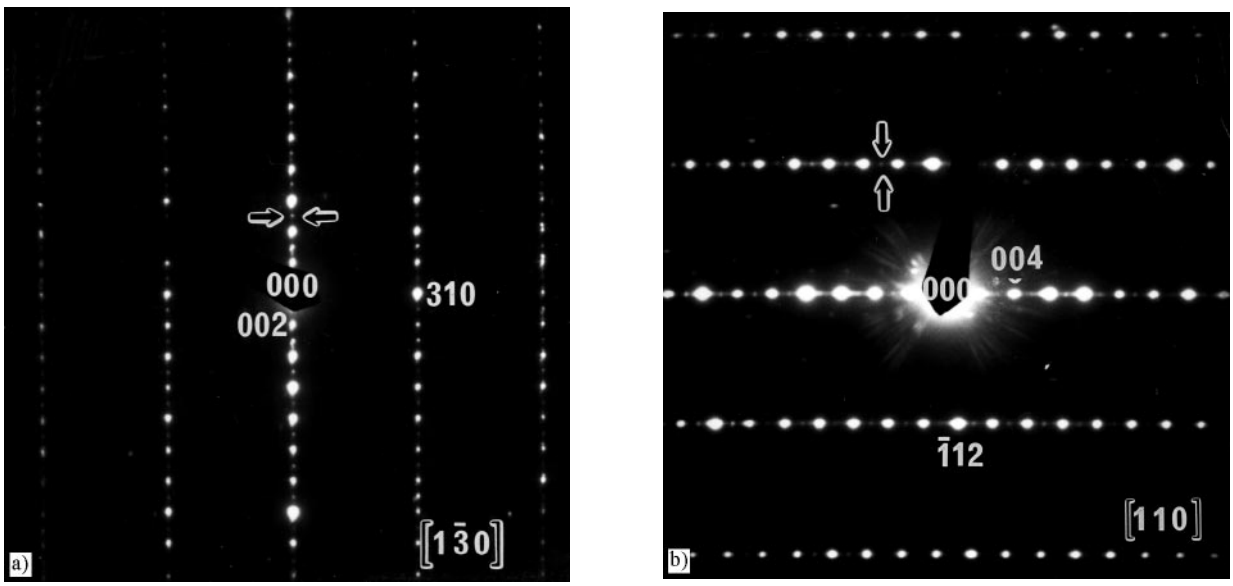

FIG. 5. Typical electron diffraction patterns showing ordering effects of samples $Na_{0.45}W_{18}O_{49}$ and $Na_{0.82}W_{18}O_{49}$. In both cases the doubling of the c parameter was needed to fully index the patterns.

Likewise, Whittingham and Huggins (22) have reported values of the order of $10^{-15}\,cm^2\,s^{-1}$ for the sodium diffusion coefficient in m-WO_3 where only quadrangular tunnels are present. These values are very different from ours and clearly indicate the difficulty of sodium ions to move along square tunnels. However, in making the comparison, we would like to note that our D values have to be taken as an approximation, since the true surface area of the electrode is not well known. The trend of our data should, however, be correct since approximately the same error should be present in the calculation made for every composition.

CONCLUSIONS

Sodium insertion in $W_{18}O_{49}$ proceeds through the formation of a solid solution in the whole range of composition ($0 \leq x \leq 1.8$). Through electrochemical methods we have detected different features in the $-\partial x/\partial E$ plot which can be associated with continuous transitions. Samples with compositions $Na_xW_{18}O_{49}$ were synthesized and characterized by electron diffraction and it was found that, for compositions close to minima in the $-\partial x/\partial E$ plot, a new ordering occurs along the c-direction. On the basis of these results we have proposed an insertion model in which ordering is present for certain compositions. We have associated this ordering with the filling of the unique hexagonal tunnel that exists in $W_{18}O_{49}$. Neutron diffraction experiments are in progress to establish the ordering at the singular compositions $x = 0.45$ and $x = 0.82$.

ACKNOWLEDGMENTS

A.M.C. thanks CONACYT (Mexico) for financial support through the J28162-E project. F.G. thanks Universidad San Pablo-CEU for supporting the projects 5/96 and 8/97. A.M.C. also thanks Dr. A. Kuhn for his kind help in the electron diffraction experiments.

REFERENCES

1. C. Julien and G. A. Nazri, "Solid State Batteries: Materials Design and Optimization," Kluwer Academic, Dordrecht, 1994.
2. W. Weppner and R. A. Huggins, *J. Electrochem. Soc.* **124,** 1569 (1977).
3. C. J. Wen, B. A. Boukamp, R. A. Huggins, and W. Weppner, *J. Electrochem. Soc.* **126,** 2258 (1979).
4. A. H. Thompson, *J. Electrochem. Soc.* **126,** 608 (1979).
5. W. R. McKinnon and J. R. Dahn, *Solid State Commun.* **48,** 43 (1983).
6. W. R. McKinnon, J. R. Dahn, J. J. Murray, R. R. Haering, R. S. McMillan, and A. H. Rivers-Bowerman, *J. Phys. C: Solid State Phys.* **19,** 5135 (1986).
7. Y. Chabre, *J. Electrochem. Soc.* **138,** 329 (1991).
8. Y. Chabre, *NATO ASI Ser.* **305,** 181 (1993).
9. Y. Chabre, *Prog. Solid State Chem.* **23,** 1 (1995).
10. A. Magnéli, *Ark. Kemi* **1,** 223 (1949).
11. K. Viswanathan, K. Brandt, and E. Salje, *J. Solid State Chem.* **36,** 45 (1981).
12. A. Martínez de la Cruz, F. García-Alvarado, E. Morán, M. A. Alario-Franco, and Leticia M. Torres-Martínez, *J. Mater. Chem.* **5**(3), 513 (1995).
13. A. Martínez de la Cruz, Leticia M. Torres-Martínez, F. García-Alvarado, E. Morán, and M. A. Alario-Franco, *Solid State Ionics* **84,** 181 (1996).
14. J. M. Tarascon, *J. Electrochem. Soc.* **132,** 2089 (1985).
15. A. Martínez de la Cruz, D. Phil. Thesis, Universidad Complutense, 1997.
16. J. R. Dahn and W. R. McKinnon, *Phys. Rev. B* **32,** 3003 (1985).
17. J. R. Dahn and W. R. McKinnon, *J. Phys. C: Solid State Phys.* **17,** 4231 (1984).
18. J. R. Dahn, W. R. McKinnon, and R. R. Haering, *Can. J. Phys.* **58,** 207 (1980).
19. R. D. Shannon and C. Prewitt, *Acta Crystallogr. B* **25,** 925 (1969); **26,** 1046 (1970).
20. F. Takusagawa and R. A. Jacobson, *J. Solid State Chem.* **18,** 163 (1976).
21. B. Schlasche and R. Schollhorn, *Rev. Chim. Mineral.* **19,** 534 (1982).
22. M. S. Whittingham and R. A. Huggins, *in* "Fast Ion Transport in Solids" (W. VanGool, Ed.), North-Holland, Amsterdam, 1973.